Mix design formulation range for metakaolin-based geopolymer synthesis

http://dx.doi.org/10.1590/0370-44672021750038

Marina Filizzola Oliveira[1,2]
https://orcid.org/0000-0002-5034-6064
Fernando Soares Lameiras[1,3]
https://orcid.org/0000-0002-3169-1647

[1]Centro de Desenvolvimento da Tecnologia Nuclear, Departamento de Minerais e Materiais, Belo Horizonte - Minas Gerais - Brasil.

E-mails: [2]filizzolamarina@gmail.com, [3]fsl@cdtn.br

Abstract

This article presents a range of mix design formulations to obtain metakaolin-based geopolymer synthesis. Geopolymer samples were synthesized from metakaolin, a 10 M sodium hydroxide solution, and alkaline sodium silicate. These three components were mixed in different proportions to form a paste which was molded in a cylindrical shape, set at room temperature for 24 hours, and demolded. The workability of the paste, the integrity of the samples, development of efflorescence, and the presence of undissolved metakaolin particles in the microstructure of the geopolymer matrix were observed. Since sodium and water play a vital role in the geopolymerization and were added at fixed proportions, a mix design was employed based on the molar proportions of aluminum, silicon, and sodium plus water. The simplex design plot was able to separate the regions of a mix of the components that showed different behaviors according to the observed responses. The dissolution of metakaolin, condensation of orthosialate and silicate species, which are expected to interact with each other according to the model of geopolymerization of Davidovits, can explain the observed results. "Good results" (no release of white powder, no efflorescence, no shrinkage, and no cracks) after 28 days of curing at room conditions were observed for the molar proportions $0.097 < Al < 0.112$, $0.120 < Si < 0.178$, and $0.711 < Na+H_2O < 0.775$ ($Na/H_2O = 0.185$).

Keywords: geopolymer, mix design, metakaolin, sodium hydroxide, sodium silicate, efflorescence.

1. Introduction

Geopolymers are made from powders of amorphous aluminosilicate materials, which are mixed with an alkaline solution usually prepared with an alkali hydroxide solution and alkaline silicate. According to Provis (2018), "alkali activation is the generic term which is applied to the reaction of a solid aluminosilicate precursor under alkaline conditions, to produce a hardened binder which is based on a combination of hydrous alkali-aluminosilicate and/or alkali-alkali earth-aluminosilicate phases. Geopolymers and alkali-activated materials are likely to have high potential to be used in common ordinary Portland cement (OPC) applications. After mixing, the obtained paste can be molded into the desired shape and hardens in a few hours. Despite the controversy whether geopolymers are alkali-activated materials or not (Provis and Bernal, 2014; Krivenko, 2017; Davidovits, 2017; Davidovits, 2018), the interest in these materials is growing because of the low CO_2 emission in their production compared to OPC (Luukkonen *et al*., 2018; Nehdi and Yassine, 2020). However, this issue depends on the regional conditions, such as energy matrix, supply and transportation of raw materials, and should be handled with care. Also, calcined clays and many industrial residues, such as silica fumes, fly ashes, calcined rice rusk, blast furnace slags, etc. (Bernal *et al*., 2016; Geraldo *et al*., 2017; Humad *et al*., 2019) can be used as aluminosilicate sources. Geopolymers have no or low content of calcium. They are also used for immobilization of fly ash from the incineration of municipal wastes (Lach *et al*., 2018) and radioactive wastes (Cantarel *et al*., 2017), and as a binder for manufacturing products for civil construction using the fine tailings from iron ore exploitation (Rodrigues *et al*., 2020).

The solid particles of the aluminosilicate powder dissolve in an alkaline solution and produce aluminate and silicate species. These species in solution and the silicate species from the alkaline solution form a complex mix of silicate, aluminate, and aluminosilicate species. Thus, a supersaturated aluminosilicate solution is formed, resulting in the formation of a gel. After gelation, the system continues to reorganize and condense in the three-dimensional framework of the hardened material (Duxson *et al*., 2007). Water is consumed in the dissolution of the aluminosilicate, but liberated in condensation. By adjusting the concentration of aluminosilicates, sodium hydroxide in solution and alkaline silicate, the Si/Al ratio, the concentration of free alkaline ions, and water in the pores of the geopolymer matrix can be controlled. Some authors claim that there is water in the three-dimensional framework of geopolymers as hydrated alkaline ions (Barbosa *et al*., 2000).

Dissolution and condensation proceed at the same time. The dissolution and condensation rate depends on the concentration, processing, and characteristics of the raw materials. If they are not balanced, not setting or too fast setting, unreacted materials, efflorescence, and cracks may be observed in the geopolymer samples. The objective of this article is to present a methodology based on mix design to establish a range of quantities of raw materials that can be used to obtain geopolymer samples with good properties. Metakaolin produced by calcination of kaolinite was employed as the aluminosilicate source.

Mix design methods for geopolymer or alkali-activated admixtures or concretes have been reported (Adbollahnejad *et al*., 2015; Phoo-ngernkham *et al*., 2018; Bellum *et al*., 2019; Ning *et al*., 2019;). De Silva *et al*. (2007) treated the initial composition of the geopolymer in a phase equilibrium diagram in molar concentration of Al_2O_3, SiO_2, and Na_2O. Oakes *et al*. (2019) reported a mix design for the composition of aluminosilicate sources for alkali-activation, but the approach presented herein is not reported to the best of our knowledge.

This article presents a range of mix design formulations to obtain metakaolin-based geopolymer synthesis to understand the influence of different component proportions as well as the molar concentration of aluminum, silicon and sodium on the behavior of produced geopolymers.

2. Materials and methods

Kaolinite of technical degree was purchased on the local market (white kaolin from Sulfal company). A 10 M solution of sodium hydroxide was prepared with tap water (from COPASA, the water supplier and distribution company in Belo Horizonte, Minas Gerais, Brazil) and sodium hydroxide of a technical degree in scales. Alkaline sodium silicate was purchased on the local market (from the Getex company, 15 wt% Na_2O, 32.20 wt% SiO_2, 47.20 wt% of solids, SiO_2/Na_2O = 2.15 by weight, 1.570 g/cm^3, 1.195 cP at 25°C, 52.9 ppm Fe content).

Metakaolin was prepared by calcination of kaolinite in a muffle furnace at 800 °C for 4 hours, with a heating rate of 10 °C/min (Elimbi *et al*., 2011) and natural cooling of the furnace to room temperature. X-ray diffractometry and Fourier transform infrared spectroscopy showed the amorphous character of the metakaolin and the absence of OH groups. The composition of metakaolin measured by X-rays fluorescence was 44.9 wt% Al_2O_3, 53.5 wt% SiO_2, 0.47 wt% K_2O, and 0.15 wt% Fe_2O_3. It is a fine white powder.

Metakaolin, sodium hydroxide solution and alkaline sodium silicate were mixed in different weight proportions, as shown in Table 1. They were manually mixed with a spatula to get a uniform paste, which was put in cylindrical molds (5 cm diameter and 10 cm height). They were vibrated for 10 minutes to eliminate air bubbles and let to set for 24 hours in room conditions and demolded with the help of a manual hydraulic press. After demolding, the samples were visually inspected every day (up to 28 days) to observe their evolution.

Water was introduced from the alkaline sodium silicate and sodium hydroxide solution. Figure 2 shows the simplex design plot in molar contents for aluminum, silicon, sodium, and water. The contents of sodium and water are highly correlated so that they were summed.

After 14 days of curing, the sample numbers 15 and 18 from Table 1 were broken by compression. Fragments of the samples were embedded in resin and polished up to a 3 µm diamond paste for scanning electron microscopy and X-rays dispersive spectroscopy, shown in Figures 4 and 5. Figure 5 shows the X-rays energy dispersive spectroscopy (EDS) map of a region of sample number 18, in which efflorescence was observed.

3. Results

The composition, molar concentration, and the results of the visual inspection of each mix produced are shown in Table 1. They were classified in the following categories: a) Extremely fast setting of the paste and because of that, the molding was impossible; b) Release of a white powder by rubbing with a finger or growth of a white mold-like layer of sodium carbonate (efflorescence); c) Good result (not classified as a, b, or d); d) Shrinkage and crack development. Figure 1 and Figure 2 show the simplex design plot for Table 1 (Montgomery, 2019). Figure 3 shows pictures of samples classified in each category.

Table 1 - Composition of the geopolymer samples (%wt), their theoretical molar concentration and observed evolution (▲: extremely fast setting; ■: white powder or efflorescence; ○: good result; ♦: shrinkage with cracks; MK: metakaolin; SS: alkaline sodium silicate; SH: 10 M sodium hydroxide solution).

Sample	Composition			Molar concentration			Evolution
	MK	SS	SH	Al	Si	$Na+H_2O$	
1	63.34	11.33	25.33	0.2	0.22	0.58	▲
2	63.30	1.40	35.30	0.19	0.22	0.59	■
3	61.50	0.00	38.50	0.19	0.19	0.61	■
4	61.70	4.60	33.70	0.19	0.21	0.6	■
5	61.70	9.60	28.70	0.19	0.23	0.59	▲
6	61.70	14.70	23.60	0.19	0.19	0.62	▲
7	60.00	3.00	37.00	0.18	0.21	0.61	■
8	60.00	8.00	32.00	0.18	0.18	0.64	■
9	60.00	13.00	27.00	0.18	0.19	0.63	■
10	60.00	20.00	20.00	0.18	0.18	0.64	▲
11	58.30	1.40	40.30	0.18	0.21	0.62	■
12	58.30	6.40	35.30	0.17	0.17	0.65	■
13	58.33	11.33	30.34	0.17	0.2	0.63	■
14	58.33	16.34	25.33	0.17	0.18	0.65	▲
15	56.70	4.60	38.70	0.17	0.19	0.64	■
16	56.70	9.70	33.60	0.17	0.17	0.66	■
17	56.70	14.70	28.60	0.17	0.18	0.65	■
18	55.00	8.00	37.00	0.16	0.17	0.67	■
19	55.00	13.00	32.00	0.16	0.18	0.66	■
20	53.33	3.33	43.34	0.16	0.17	0.67	■
21	53.33	18.33	28.34	0.15	0.19	0.66	▲
22	51.67	16.67	31.66	0.15	0.19	0.67	▲
23	51.67	21.67	26.66	0.15	0.15	0.7	▲
24	50.00	0.00	50.00	0.15	0.2	0.66	○
25	50.00	10.00	40.00	0.15	0.17	0.68	○
26	50.00	13.00	37.00	0.14	0.17	0.68	■
27	50.00	15.00	35.00	0.14	0.16	0.7	■
28	50.00	20.00	30.00	0.14	0.16	0.7	▲
29	50.00	30.00	20.00	0.14	0.2	0.66	○
30	48.33	18.33	33.34	0.14	0.15	0.71	■
31	48.33	23.33	28.34	0.13	0.17	0.69	▲
32	46.66	16.66	36.68	0.13	0.13	0.74	○
33	46.67	6.67	46.66	0.13	0.16	0.71	■
34	46.66	21.67	31.67	0.13	0.17	0.7	▲
35	46.67	26.67	26.66	0.13	0.16	0.71	○
36	46.67	36.67	16.66	0.13	0.15	0.72	○
37	45.00	20.00	35.00	0.12	0.2	0.67	■
38	43.33	3.33	53.34	0.12	0.13	0.75	○

39	43.33	13.33	43.34	0.12	0.15	0.73	○
40	43.34	23.33	33.33	0.12	0.17	0.71	▲
41	43.34	26.66	30.00	0.12	0,17	0.72	○
42	43.34	30.00	26.66	0.12	0.16	0.72	○
43	43.34	33.33	23.33	0.12	0.15	0.73	○
44	40.00	10.00	50.00	0.11	0.2	0.69	○
45	40.00	20.00	40.00	0.11	0.13	0.76	○
46	40.00	26.67	33.33	0.11	0.17	0.72	○
47	40.00	30.00	30.00	0.11	0.11	0.78	○
48	40.00	33.33	26.67	0.11	0.16	0.73	○
49	40.00	40.00	20.00	0.11	0.15	0.74	○
50	40.00	50.00	10.00	0.1	0.15	0.75	○
51	39.00	25.00	36.00	0.1	0.16	0.74	○
52	39.00	36.00	25.00	0.1	0.13	0.76	○
53	36.67	30.00	33.33	0.1	0.14	0.76	○
54	36.67	33.33	30.00	0.1	0.11	0.79	○
55	36.67	36.67	26.66	0.1	0.15	0.75	○
56	33.33	23.33	43.34	0.09	0.15	0.76	♦
57	33.33	33.33	33.34	0.09	0.14	0.77	♦
58	33.33	53.33	13.34	0.09	0.13	0.78	♦
59	36.67	26.67	36.66	0.09	0.17	0.74	○
60	30.00	40.00	30.00	0.09	0.15	0.76	♦
61	30.00	20.00	50.00	0.08	0.13	0.78	○
62	30.00	50.00	20.00	0.08	0.11	0.81	♦

The simplex design plot in concentration (wt %) shown in Figure 1 clearly separates the regions of different results. Most of the "Good results" were observed where the quantity of metakaolin was between 37 and 50 wt%, and the alkaline sodium silicate was higher than 25 wt%. It seems that there is a region perpendicular to the base of the triangle where the results are "Extremely fast setting". It is delimited by the region where the content of metakaolin was between 43 and 63 wt% and the content of alkaline sodium silicate between 11 and 20 wt%. The results "White powder or efflorescence" were observed where the content of metakaolin was higher than 45 wt% and the content of alkaline sodium silicate less than 20 wt%. Samples with metakaolin lower than 33.33 wt% and alkaline sodium silicate higher than 23.33 wt% developed shrinkage or cracks.

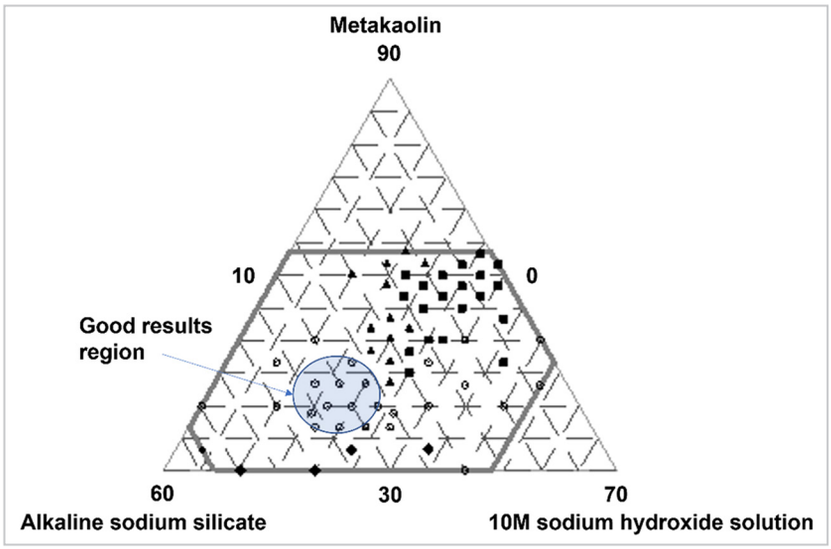

Figure 1 - Simplex design plot for Table 1. Components in %wt.
▲- Extremely fast setting; ■ - White powder or efflorescence; ○ – Good result; ♦ - Shrinkage with cracks.

The simplex design plot in molar concentration (Figure 2) also separates the regions of different results. The results "Extremely fast setting" are close to the diagonal of the rhombus for the molar concentration of aluminum greater than 0.120. The results "White powder or efflorescence" are above the diagonal of the rhombus, and most of the "Good results"

are below this diagonal for the molar concentration of aluminum greater than 0.09. "Shrinkage with cracks" were observed for molar concentration of aluminum less than 0.09.

Undissolved metakaolin and Na^+ dissolved in water inside pores in the matrix of geopolymer may explain the observation of "White powder and efflorescence". Figures 4 and 5 show undissolved metakaolin (related to the regions of high concentration of aluminum) and a high concentration of sodium in some spots. Figure 5 shows the efflorescence in the pores in sample number 18, point 2. The distribution of carbon and sodium are similar, indicating the micro-formation of sodium carbonate in the pores. The elemental composition of Spots 1 and 2, identified by X-ray energy dispersive spectroscopy (EDS), were shown in Table 2.

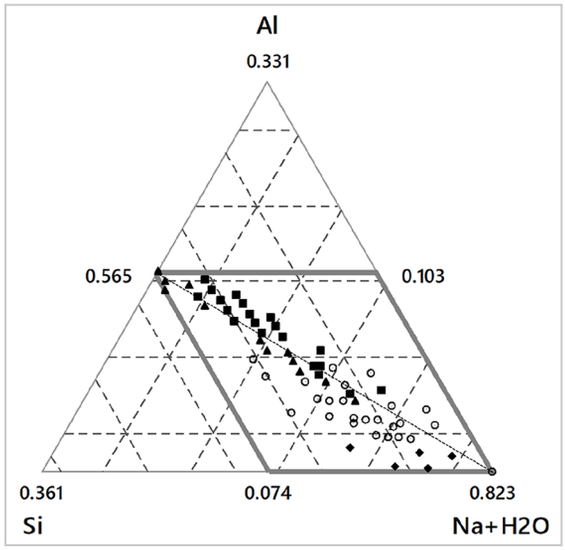

Figure 2 - Simplex design plot for Table 1 in molar concentration.
▲- Extremely fast setting; ■ - White powder or efflorescence; ○ – Good result; ♦ - Shrinkage with cracks.

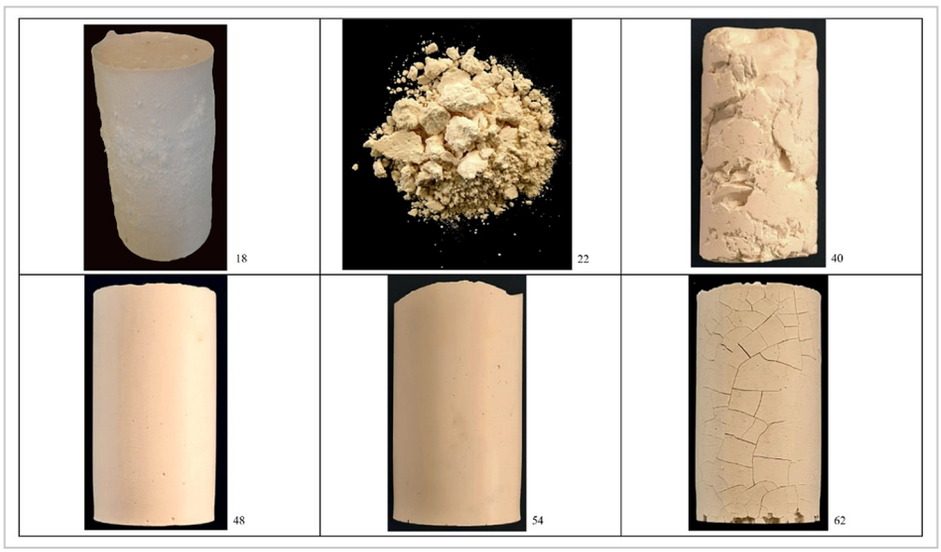

Figure 3 - Pictures of the geopolymer samples, according to the sample number of Table 1.
Sample number 18 is a case of "White powder or efflorescence". Samples 22 and 40 are cases of "Extremely fast setting". Sample 22 set during the mixing. Samples 48 and 54 are cases of "Good result". Sample 62 is a case of "Shrinkage with cracks".

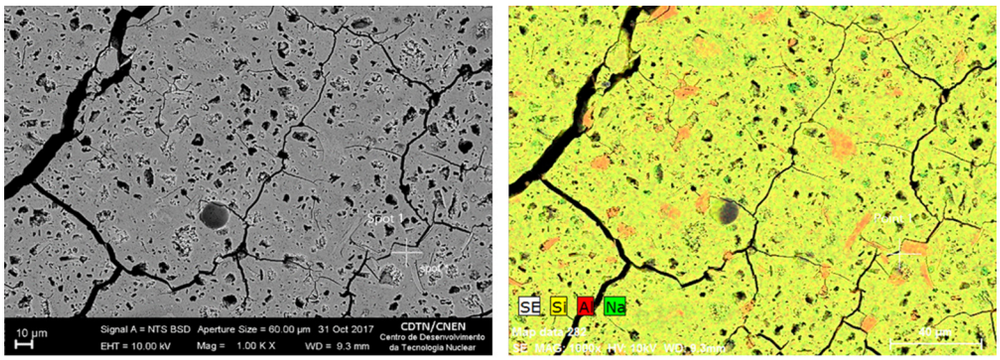

Figure 4 - Scanning electron microscopy (left) and X-rays dispersive spectroscopy map (right) of sample number 15 of Table 1.

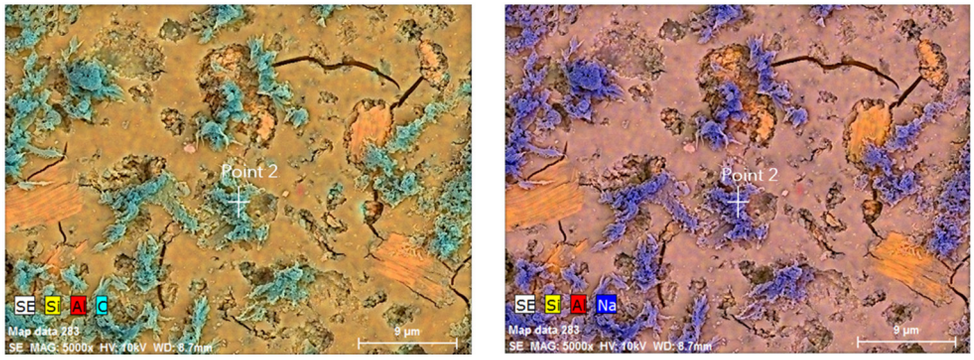

Figure 5 - X-rays dispersive spectroscopy map in a region of sample number 18 of Table 1, showing the distribution of carbon and sodium (sodium carbonate formation).

Table 2 - EDS spots for the samples 15 (point 1) and 18 (point 2).

Element	Point 1	Point 2
	Wt. %	Wt. %
C	-	52.9
O	63.0	33.8
Na	10.9	10.3
Si	16.9	2.0
Al	8.1	0.9

4. Discussion

In a sodium alkaline solution, geopolymerization occurs in the steps shown in Figures 6 to 11 according to Davidovits (2017). Water and Na^+ are fixed in the ortho-sialate species in steps 1 to 5. The sixth step is condensation, when the ortho-sialate molecules combine, liberating Na^+ and OH^- for performing steps 1 to 5 again. Figure 11 shows two possible combinations of ortho-sialate molecules.

Water is particularly important for geopolymeratization, although it is not consumed at the end. It provides the means for the dissolution of metakaolin and the transport and rearrangement of ortho-sialate molecules, silicate species, and Na^+ and OH^- ions. Water is also important for the workability of the paste resulted from the mix of metakaolin, sodium hydroxide solution, and alkaline sodium silicate.

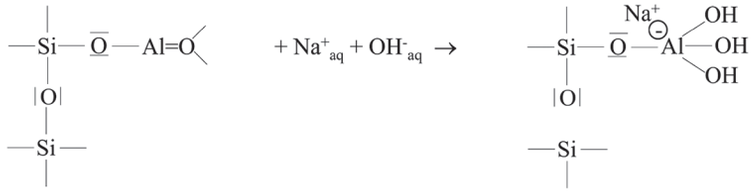

Figure 6 - First step: Formation of tetravalent Al in the group sialate -Si-O-Al-$(OH)_3$-Na^+. Adapted from Davitovits (2017).

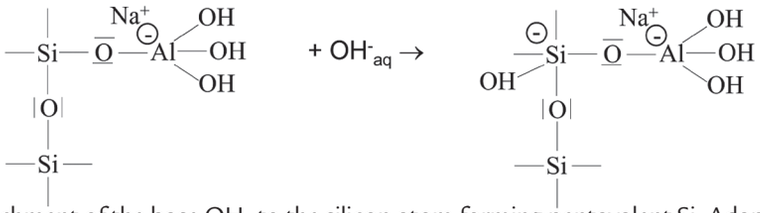

Figure 7 - Second step: Attachment of the base OH- to the silicon atom forming pentavalent Si. Adapted from Davitovits (2017).

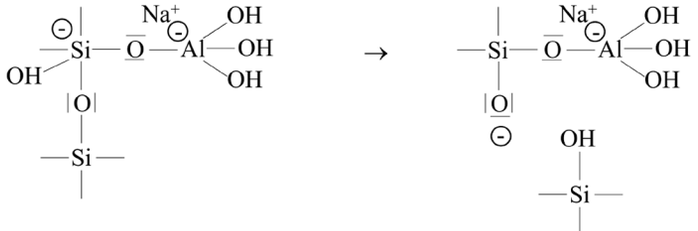

Figure 8 - Third step: Cleavage of the siloxane oxygen in Si-O-Si through transfer of the electron from Si to O, formation of intermediate silanol Si-OH on the one hand, and siloxo Si-O- on the other hand. Adapted from Davitovits (2017).

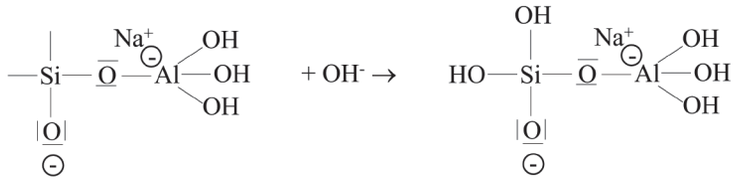

Figure 9 - Fourth step: Further formation of silanol Si-OH groups and isolation of the ortho-sialate molecule, the primary unit in geopolymerization. Adapted from Davitovits (2017).

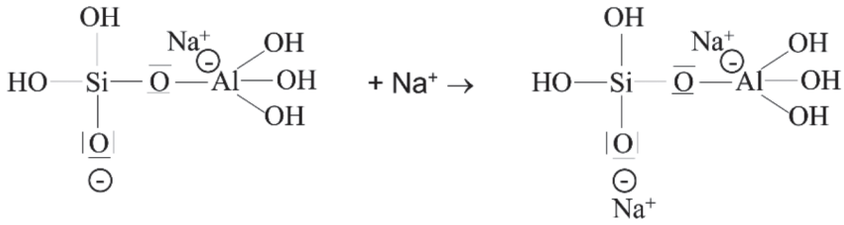

Figure 10 - Fifth step: Formation of Si-O-Na terminal bond, with attachment of a Na^+ ion, forming an ortho-sialate molecule. Adapted from Davitovits (2017).

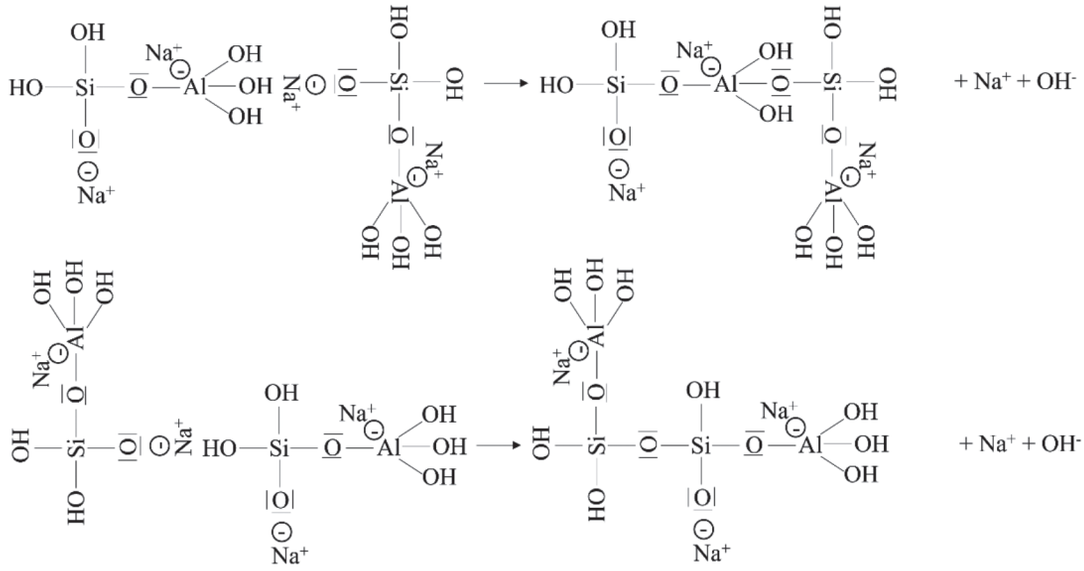

Figure 11 - Sixth step: Possible combinations of ortho-sialate molecules during condensation Adapted from Davitovits (2017).

When there is alkaline sodium silicate in the solution, different silicate species can exist. Q^x denotes the connectivity of the species, where x is the number of neighboring Si atoms of a given Si atom. Figure 12 shows the Q^1, but Q^1 to Q^4 can coexist depending on the modulus n in the formula $Na_2O.nSiO_2$ of the alkaline sodium hydroxide (Jansson *et al.*,2015). In principle, every Si-O-Na end of the dissolved species can participate in condensation.

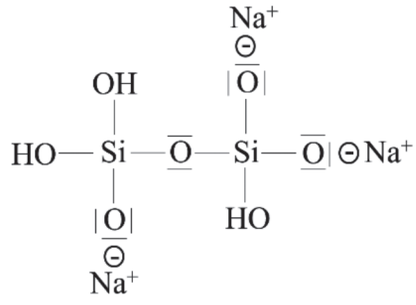

Figure 12 - Q^1 species of silicate in alkaline sodium hydroxide. Adapted from Davitovits (2017).

Na^+ is important for the dissolution of metakaolin into ortho-sialate molecules (Figures 6 to 11). It is consumed because every aluminum atom in the ortho-sialate molecules and in the geopolymer structure should be charge-compensated by a sodium ion. Another Na+ ion is attached to the ≡Si-O· end. It is liberated in the condensation and can participate once again in the dissolution of metakaolin (Figure 12).

The increase in the concentration of ortho-sialate molecules in the solution

increases the condensation rate. So, there is an interaction between the dissolution of metakaolin and the condensation. During the dissolution of metakaolin, the concentration of Na^+ and water decreases. Then, the rate of dissolution should decrease. If the molar relation Na/Al is less than 1, the sodium can be totally consumed and part of the metakaolin cannot be dissolved. If the Na/Al is 1, the dissolution can be completed, but in a long time, provided there is available water. If it is higher than 1, there will be enough Na+ to sustain the dissolution, provided there is available water, and it is expected that the geopolymerization will proceed at higher rates. But in the end excess sodium will be in the geopolymer matrix, which may cause efflorescence (Zuhua *et al.*, 2018).

The Si/Al ratio is also important because when it is higher than 1, more Q^x species of silicate will be in solution to increase the condensation rate. It is achieved by the addition of sodium silicate (Figure 12). But if the condensation rate increases too much in relation to the dissolution rate, parts of the geopolymer matrix will be set, expelling water to the regions of no condensation, decreasing the Na+ concentration in these regions and the dissolution rate. So, parts of the geopolymer matrix will remain with undissolved metakaolin.

Because of the interaction between the dissolution and condensation, the ideal mix of metakaolin, alkaline sodium silicate, and solution of sodium hydroxide is not a trivial issue for geopolymer synthesis. Undissolved metakaolin, unreacted alkaline sodium silicate or sodium hydroxide may result in the geopolymer matrix.

The complex behavior of the geopolymerization process was described by Xiao *et al.* (2009) based on isothermal calorimetry characterization. The geopolymerization reaction was also studied by Qian *et al.* (2017). Provis and Deventer (2007) proposed a model for the kinetics of geopolimerization based on the dissolution of metakaolin in silicate and aluminate monomers, the addition of polymerized silicate species from the activation solution, formation of aluminosilicate oligomers, and subsequent formation of amorphous aluminosilicate polymer and amorphous aluminosilicate gel.

Figure 13 shows how geopolymerization takes place from the microstructural point of view. In the beginning, the solid metakaolin particles are in the alkaline solution. Dissolving these particles releases ortho-sialate species that fix water and Na^+ ions (Figure 13a). As the concentration of the ortho-sialate species increases in the solution, condensation begins, with the formation of geopolymer particles, with the release of water and Na^+ ions (Figure 13b). The geopolymer particles incorporate Na^+ ions, such that their concentration in the alkaline solution decreases. The lower concentration of Na^+ in solution decreases the rate of dissolution of the metakaolin particles. In this process, the metakaolin particles decrease in size and the geopolymer particles grow (Figure 13c and 13d). As they grow, the geopolymer particles begin to coalesce, forming pores filled with solution and surrounding the metakaolin particles (Figure 13e). Eventually, the metakaolin particles can become completely enveloped by the geopolymer matrix and no longer dissolve. The solution trapped in the pores may contain Na^+ in solution and cause efflorescence. The pores can be opened or closed.

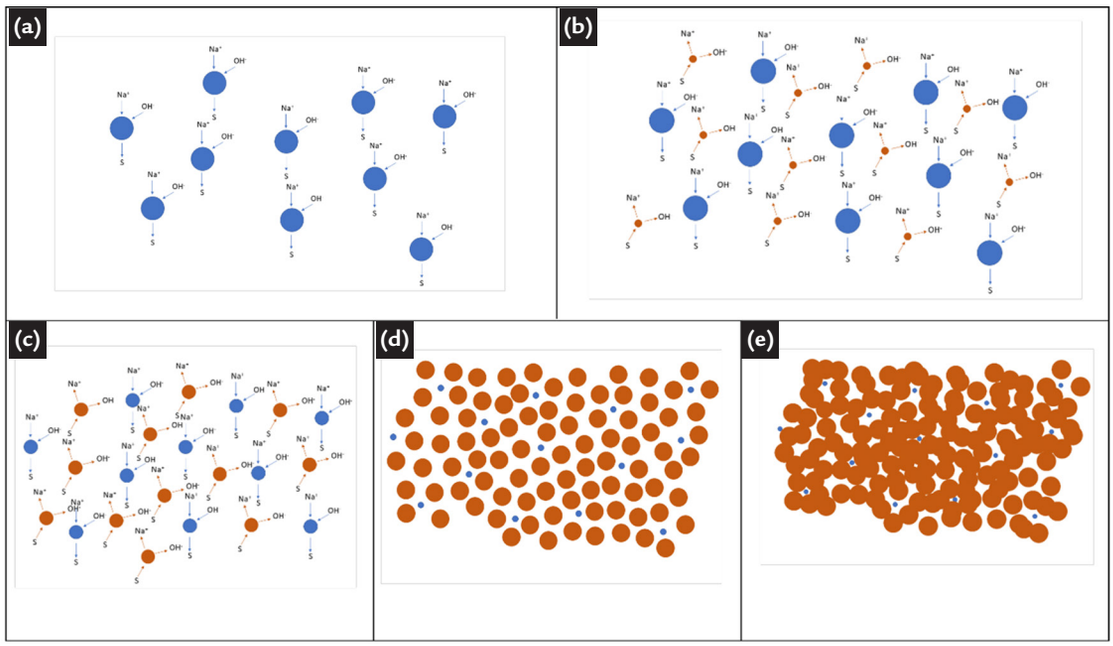

Figure 13 - Depiction of the geopolimerization process.
S represents the ortho-sialate species, • is a metacaulim particle, and • is a geopolymer particle.

In an ideal situation, if the Na/Al ratio ≈ 1 and the dissolution and condensation rates allow the complete dissolution of the metakaolin particles, water will remain in the porosity of the geopolymeric matrix. If the dissolution rate is high, the condensation rate will also be high. In this case, the geopolymer particles can grow and coalesce, surrounding the metakaolin particles and form pores with Na+ in solution. Rapid setting with undissolved particles of metakaolin and efflorescence may be observed. If the dissolution rate is low, the condensation rate will also be low. This is a case where setting can be slow and the metakaolin particles may not be completely dissolved. The pores will be filled with Na^+ in solution and lead to efflorescence. If the Na/Al ratio > 1, there will always be Na^+ ions in the residual solution trapped in the pores, with the consequent development of efflorescence. The higher Na+ concentration increases the dissolution and condensation rates and can lead to the situation with metakaolin particles not completely dissolved. If the Na/Al ratio <1, there will not be enough sodium

to dissolve the metakaolin completely and the dissolution and condensation rates will be slow. Metakaolin particles will result in the geopolymer matrix.

The Si/Al ratio also has an influence. Metakaolin has Si/Al = 1. The Si/Al ratio > 1 is the result of adding sodium silicate to the solution. This addition increases the Na^+ content in the solution and the dissolution rate. The condensation rate also increases, due to the higher content of silicate species. For greater additions of sodium silicate, cracks in the surfaces in the samples and shrinkage of the samples were observed.

In summary, several factors can influence the dissolution rate of metakaolin particles and condensation rates. Besides the characteristics of metakaolin (composition, granulometry, and calcination conditions), the concentration and composition of the alkaline solution, as well as the conditions of setting (at room temperature or at a higher temperature, air moisture and time) influence on these rates. Unbalanced rates of dissolution and condensation may result in undissolved metakaolin and Na^+ in solution trapped in the pores of the geopolymeric matrix, causing the "white powder", efflorescence, fast setting, and cracks in the geopolymer samples. A simplex design of raw materials mix, visual inspections as shown in Figure 1 and 2, and MEV/EDS maps like the one shown in Figures 4 and 5 may be helpful to identify these problems.

5. Conclusions

Geopolymer samples were synthesized from a mix of metakaolin, alkaline sodium silicate, and 10 M sodium hydroxide solution. Mixes of different concentration of these components were studied. It was mixed to form a paste then molded, vibrated, set at room conditions, and demolded after 24 hours. The workability of the paste, the integrity of the samples, and the development of efflorescence was observed by visual inspection of the samples for 28 days of curing at room conditions. It was classified as "white powder or efflorescence", "extremely fast setting", "good result", or "shrinkage with cracks". The simplex design plot in wt% of the components as well as in molar concentration of aluminum, silicon, and sodium plus water can separate the regions where these results can be classified.

These results were explained based on the Davidovits geopolymerization model with qualitative consideration of the dissolution rates of metakaolin and condensation of ortho-sialate molecules and silicate species from alkaline sodium silicate. The dissolution of metakaolin and the condensation of ortho-sialate and silicate species interact with each other. The Na^+ plays an important role both in dissolution and condensation. Water, although not consumed in geopolymeration, is especially important to promote the medium for transportation and rearrangement of ortho-sialate molecules, silicate species, and Na^+ ions. The process of geopolymerization was also described from the microstructural point of view.

The ideal mix of metakaolin, alkaline sodium silicate, and solution of sodium hydroxide is not a trivial issue for geopolymer synthesis. Undissolved metakaolin or unreacted alkaline sodium silicate or sodium hydroxide may result in the geopolymer matrix causing the release of white powder by friction, efflorescence, fast setting, and cracks. A simplex design of raw material mix, visual inspections and MEV/EDS maps may be helpful to avoid these problems. "Good results" (no release of white powder, no efflorescence, no shrinkage, and no cracks) after 28 days of curing at room conditions were observed for the molar proportions $0.097 < Al < 0.112$, $0.120 < Si < 0.178$, and $0.711 < Na+H_2O < 0.775$ ($Na/H_2O = 0.185$).

Acknowledgements

To CAPES, FAPEMIG, CNPq, INCT Midas, and Samarco Mineração S. A.

References

ABDOLLAHNEJAD, Z.; PACHECO-TORGAL, F.; FÉLIX, T.; TAHRI, W.; BARROSO AGUIAR, J. Mix design, properties and cost analysis of fly ash-based geopolymer foam. ***Construction and Building Materials***, v. 80, p. 18-30, 2015.

BARBOSA, V. F. F; MACKENZIE, K. J. D; THAUMATURGO, C. Synthesis and characterisation of materials based on inorganic polymers of alumina and silica: sodium polysialate polymers. ***International Journal of Inorganic Materials***, v. 2, n. 4, p. 309-317, 2000.

BELLUM, R. R.; NERELLA, R; MADDURU, S. R. C.; INDUKURI, C. S. R. Mix design and mechanical properties of fly ash and GGBFS-synthesized alkali-activated concrete (AAC). ***Infrastructures***, v. 4, n. 2, p. 20, 2019.

BERNAL, S. A.; RODRÍGUEZ, E. D.; KIRCHHEIM, A. P.; PROVIS, J. L. Management and valorisation of wastes through use in producing alkali-activated cement materials. ***Journal of Chemical Technology & Biotechnology***, v. 91, n. 9, p. 2365-2388, 2016.

CANTAREL, V.; MOTOOKA, T.; YAMAGISHI, I. ***Geopolymers and their potential applications in the nuclear waste management field-a bibliographical study.*** Tokai-mura, Naka-gun, Ibaraki-ken:Japan Atomic Energy Agency, 2017. 48p. (JAEA-Review 2017-014 report).

DAVIDOVITS, J. Geopolymers: ceramic-like inorganic polymers. ***Journal of Ceramic Science and Technology***, v. 8, n. 3, p. 335-350, 2017.

DAVIDOVITS, J. Why alkali-activated materials (AAM) are not geopolymers. ***Publication Technical Paper***, v. 25, 2018.

DE SILVA, P.; SAGOE-CRENSTIL, K.; SIRIVIVATNANON, V. Kinetics of geopolymerization: role of Al_2O_3 and SiO_2. Cement and Concrete Research, v. 37, n. 4, p. 512-518, 2007.

DUXSON, P. *et al*. Geopolymer technology: the current state of the art. ***Journal of materials science***, v. 42, n. 9,

p. 2917-2933, 2007.
ELIMBI, A.; TCHAKOUTE, H. K.; NJOPWOUO, D. Effects of calcination temperature of kaolinite clays on the properties of geopolymer cements. ***Construction and Building Materials***, v. 25, n. 6, p. 2805-2812, 2011.
GERALDO, R. H.; OUELLET-PLAMONDON, C. M.; MUIANGA, E. A. D.; CAMARINI, G. Alkali-activated binder containing wastes: a study with rice husk ash and red ceramic. ***Cerâmica***, v. 63, n. 365, p. 44-51, 2017.
HUMAD, A. M.; KOTHARI, A.; PROVIS, J. L.; CWIRZEN, A. The effect of blast furnace slag/fly ash ratio on setting, strength, and shrinkage of alkali-activated pastes and concretes. ***Frontiers in Materials***, v. 6, p. 9, 2019.
JANSSON, H.; BERNIN, D.; RAMSER, K. Silicate species of water glass and insights for alkali-activated green cement. ***Aip Advances***, v. 5, n. 6, p. 067167, 2015.
KRIVENKO, P. Alkali activated cements versus geopolymers. ***Civil Engineering Research Journal***, v. 1, n. 5, 2017.
ŁACH, M.; MIERZWIŃSKI, D.; KORNIEJENKO, K.; MIKUŁA, J.; HEBDA, M. Geopolymers as a material suitable for immobilization of fly ash from municipal waste incineration plants. ***Journal of the Air & Waste Management Association***, v. 68, n. 11, p. 1190-1197, 2018.
NING, L.; CAIJUN, S.; ZUHUA, Z.; HAO, W.; YIWEI, L. A review on mixture design methods for geopolymer concrete. ***Composites Part B: Engineering***, v. 178, p. 107490, 2019.
LUUKKONEN, T.; ABDOLLAHNEJAD, Z.; YLINIEMI, J.; KINNUNEN, P.; ILLIKAINEN, M. One-part alkali-activated materials: A review. ***Cement and Concrete Research***, v. 103, p. 21-34, 2018.
MONTGOMERY, D. C. Design and analysis of experiments. 10th. ed. Hoboken: John wiley & sons, 2019.
NEHDI, M. L.; YASSINE, A. Mitigating portland cement CO_2 emissions using alkali-activated materials: system dynamics model. ***Materials***, v. 13, n. 20, p. 4685, 2020.
OAKES, L.; MAGEE, B.; MCILHAGGER, A.; MCCARTNEY, M. Strength prediction and mix design procedures for geopolymer and alkali-activated cement mortars comprising a wide range of environmentally responsible binder systems. ***Journal of Structural Integrity and Maintenance***, v. 4, n. 3, p. 135-143, 2019.
PHOO-NGERNKHAM, T. *et al*. A mix design procedure for alkali-activated high-calcium fly ash concrete cured at ambient temperature. ***Advances in Materials Science and Engineering***, v. 2018, 2018.
PROVIS, J. L. Alkali-activated materials. ***Cement and Concrete Research***, v. 114, p. 40-48, 2018.
PROVIS, J. L.; BERNAL, S. A. Geopolymers and related alkali-activated materials. ***Annual Review of Materials Research***, v. 44, p. 299-327, 2014.
PROVIS, J. L.; VAN DEVENTER, J. S. J. Geopolymerisation kinetics. 2. Reaction kinetic modelling. ***Chemical engineering science***, v. 62, n. 9, p. 2318-2329, 2007.
RODRIGUES, M. *et al*. The Use of Iron Ore Tailings in the Iron Quadrangle of Minas Gerais, Brazil. ***KnE Engineering***, p. 147–156, 2020.
XIAO, Y.; ZUHUA, Z.; HUAJUN, Z.; YUE, C. Geopolymerization process of alkali–metakaolinite characterized by isothermal calorimetry. ***Thermochimica Acta***, v. 493, n. 1-2, p. 49-54, 2009.
QIAN, W. *et al*. Geopolymerization reaction, microstructure and simulation of metakaolin-based geopolymers at extended Si/Al ratios. Cement and Concrete Composites, v. 79, p. 45-52, 2017.
ZUHUA, Z.; PROVIS, J. L.; XUE, M.; REID, A.; HAO W. Efflorescence and subflorescence induced microstructural and mechanical evolution in fly ash-based geopolymers. ***Cement and Concrete Composites***, v. 92, p. 165-177, 2018.

Received: 2 August 2021 - Accepted: 13 March 2022.